Metallophysics and Advanced Technologies
Металофіз. новітні технол.
Metallofiz. Noveishie Tekhnol.
2023, vol. 45, No. 10, pp. 1141–1150
https://doi.org/10.15407/mfint.45.10.1141
Reprints available directly from the publisher

PACS numbers: 74.45.+c, 74.55.+v, 74.70.Ad, 75.50.Cc, 75.70.Cn

Proximity Effect between a Two-Band Superconductor and a Ferromagnet

I. Martynenko[*], O. Kalenyuk[*,**], A. Shapovalov[*,**], H. Kondakova[**], V. Shamaev[***], O. Boliasova[**,****], and O. Zhitlukhina[**,****]

[*]*G. V. Kurdyumov Institute for Metal Physics, N.A.S. of Ukraine, 36 Academician Vernadsky Blvd., UA-03142 Kyiv, Ukraine*
[**]*Kyiv Academic University, N.A.S. and M.E.S. of Ukraine, 36 Academician Vernadsky Blvd., UA-03142 Kyiv, Ukraine*
[***]*Donetsk National Technical University, 2 Shybankov Sqr., UA-85300 Pokrovs'k, Ukraine*
[****]*Donetsk Institute for Physics and Engineering. Named after O. O. Galkin, N.A.S. of Ukraine, 46 Nauky Ave., UA-03028 Kyiv, Ukraine*

The proximity effect in heterostructures formed by the superconducting and ferromagnetic metals is one of the central problems of fundamental metal physics, the solution of which will make it possible to obtain new non-reciprocal electronic components and detectors of electromagnetic radiation. In this work, we create and study point contacts between the two-band superconductor Mo–Re alloy and the strong ferromagnet Ni. We confirm theoretical conclusions about the significant impact of relatively small changes in interface resistance on the current–voltage characteristics of the hybrid contact and discover different degrees of the ferromagnetic electrode effect on two fundamentally distinct superconducting subsystems. The obtained results are useful for developing new hybrid devices based on multiband superconductors.

Corresponding author: Andriy Petrovych Shapovalov
E-mail: shapovalovap@gmail.com

Citation: I. Martynenko, O. Kalenyuk, A. Shapovalov, H. Kondakova, V. Shamaev, O. Boliasova, and O. Zhitlukhina, Proximity Effect between a Two-Band Superconductor and a Ferromagnet, *Metallofiz. Noveishie Tekhnol.*, **45**, No. 10: 1141–1150 (2023). DOI: 10.15407/mfint.45.10.1141

Key words: hybrid heterostructures, two-band superconductor, strong ferromagnet, proximity effect.

Ефект близькости у гетероструктурах, утворених надпровідними та феромагнетними металами, є однією з центральних проблем фундаментальної металофізики, вирішення якої уможливить одержати нові невзаємні електронні компоненти та детектори електромагнетного випромінення. У цій роботі ми створили та дослідили точкові контакти між двозонним надпровідним стопом Mo–Re і сильним феромагнетиком Ni. Підтверджено теоретичні висновки про істотний вплив відносно невеликих змін опору роздільчої межі на вольт-амперні характеристики гібридного контакту та виявлено різного ступеня дію феромагнетної електроди на дві принципово відмінні надпровідні підсистеми. Одержані результати стануть корисними для розробки нових гібридних пристроїв на основі багатозонних надпровідників.

Ключові слова: гібридні гетероструктури, двозонний надпровідник, сильний феромагнетик, ефект близькости.

(Received 2 October, 2023; in final version, 20 October, 2023)

1. INTRODUCTION

The presence of several electronic bands at the Fermi level is a feature of most superconductors, but, due to the fairly strong interband interaction, the energy gap extends over a narrow range of magnitudes and, therefore, can be characterized by a single value Δ. In conventional BCS superconductors, the tunnelling conductance G *vs.* voltage V spectra reach a maximum at $V = \Delta/e$, while the corresponding point contact characteristics have a plateau at bias voltages $V < \Delta/e$, the value of which is equal to twice the normal-state conductance $G_N = 1/R_N$ where R_N is the contact resistance at large voltages $V >> \Delta/e$. In 2001, it became evident that a two-band–two-gap model proposed earlier in 1959 [1] may be directly applied to magnesium diboride MgB_2, a superconductor with a nearly twice critical temperature compared to the traditional Nb-based superconductors and high upper critical fields. The specific of this compound is associated with a fundamentally distinct character of the bands opening on Fermi-surface parts and their linking via comparatively weak interband coupling. It is just the case of the system where, as was shown in Ref. [1], the critical temperature T_c should be higher than the corresponding values for individual bands. Even more, an increased number of degrees of freedom may generate novel phenomena relating the responses to external perturbations absent in single-band superconductors, for example, collective excitations predicted by Leggett [2], which are corresponding to the motion of the relative phase of two superfluid components with the Josephson interband coupling between them.

The presence of two gaps has been experimentally confirmed in several other superconducting materials, such as Nb-doped $SrTiO_3$ [3], pnictide superconductors [4, 5], and Mo–Re alloy [6–8]. Despite the relatively large number of publications devoted to the unusual properties of systems based on two-gap superconductors, a number of experimental issues, including the proximity effect between dirty two-band superconductors (S) and ferromagnets (F), remain unclear. As was shown theoretically [9], intensive interband scattering in the F layer creates lot of differences from the single-band results. The condensate functions penetrating the F layer continue to be coupled although the coupling strength is suppressed by the exchange field and modulated by the diffusion coefficients of the two bands. It relates also the superconductor where two subsystems are now coupled through the proximity effect as well. When the exchange field is inhomogeneous, odd-frequency triplet superconductivity is arising. The triplet superconducting correlations with nonzero projection in the direction of the exchange field can penetrate into the F layer over large distances without any oscillations. This type of triplet superconductivity was studied in composites of MgB_2 granules with grains of manganites, half-metallic ferromagnets [10–12], while, in Ref. [13], the influence of nanoparticle geometrical and percolation effects on the electrical transport through such nanocomposites was revealed and, in Ref. [14], the role of inelastic scatterings across the contacts with manganites was emphasized.

In the present work, Andreev spectra of point contacts between superconductors and strongly spin-polarized ferromagnets with two-band properties were studied. Following the work [15], we will pay attention to the properties of the interface region and emphasize the importance of spin mixing caused by interface scattering, crucial for the creation of exotic pairing correlations in such structures. The main conclusion of Ref. [15] is that the shape of the interfacial potential has a very strong influence on the magnitude of the spin-mixing effect.

The analysis of the measured curves is based on the oversimplified Blonder–Tinkham–Klapwijk (BTK) approach [7, 8] employed to fit experimental data of S/F point-contact spectra with the interface being described by a single parameter $Z = U_0 / (\hbar v_F)$ related to its transparency, where $U_0\delta(x)$ is the effective potential localized at the interface, and v_F is the Fermi velocity. The second important fitting quantity is the so-called Dynes parameter Γ determined by the conditions of sample preparation and the temperature of the experiment [7, 8]. When the normal counter-electrode is ferromagnetic, it should be noticed that its spin polarization is not a bulk property, as was often assumed, but at least partially an interface characteristic [16].

In the next section, we discuss the main properties of the conductors forming the point contact, namely, ferromagnetic nickel and Mo–Re

alloy with approximately equal concentrations of molybdenum and rhenium as well as their characterization. Next, we describe the creation of point contacts between them, the results of electrical measurements and compare the differential conductance spectrum with the theoretically expected one. The paper ends with a discussion of the findings and conclusions.

2. POINT-CONTACT MATERIALS

The Mo–Re alloy is known to be a type II superconductor with a high upper critical field of 8 T at 4 K and a critical temperature T_c up to 15 K. Mo–Re thin films are relatively easy to produce by magnetron sputtering, have little oxidation under ambient conditions, and are suitable for electron beam lithography. For this reason, this alloy is increasingly used in superconducting devices.

From the fundamental point of view, Mo–Re alloys is an excellent example of the statement that in alloys with high concentrations of scattering centres small variations in the density of electronic states can introduce pronounced effects. Indeed, the addition of Re impurities to pure Mo led to a growth in the electron concentration, thereby bringing the Fermi level of the system closer to the critical energies of the electronic spectrum of molybdenum [17]. As a result, a transformation of the electron spectrum takes place, namely, the appearance of a new Fermi-surface cavity of $\cong 10$ at.% of a Re concentration and then partial localization of electrons belonging to the new d group. It leads to softening of the phonon spectrum in Mo–Re alloys and an enhancement of the electron–phonon interaction detected by the point-contact spectroscopy study [18]. Most probably, it is the main source of the T_c increase to about 15 K and the appearance of a second energy gap in the spectrum of quasi-particle states in a Mo–Re superconductor. In our paper [6], we demonstrated the presence of two gaps in the $Mo_{0.65}Re_{0.35}$ alloy by tunnelling spectroscopy. The values $\Delta l = 2.5$ meV and $\Delta s = 0.5$ meV found by us in Ref. [6] were in good agreement with 2.3 meV and 0.7 meV as well as with 1.9 meV and 0.5 meV for a $Mo_{0.6}Re_{0.4}$ alloy obtained by other authors [19]. In the next publication [7], we presented point-contact evidences of the presence of two significantly distinct energy gaps $\Delta l = 1.65$ meV and $\Delta s = 0.55$ meV with the dominant contribution of the band with a smaller gap in a Mo–Re alloy with approximately equal component concentrations. In the paper [8], the presence of the two gaps was confirmed by revealing bosonic, undamped collective modes and their harmonics, which were identified as manifestation of a Leggett mode arising due to relative phase fluctuations between two superconducting order parameters. In all previous point-contact experiments, we were dealing with contacts formed by a silver tip and a Mo–Re alloy film. In the new work, we fundamentally

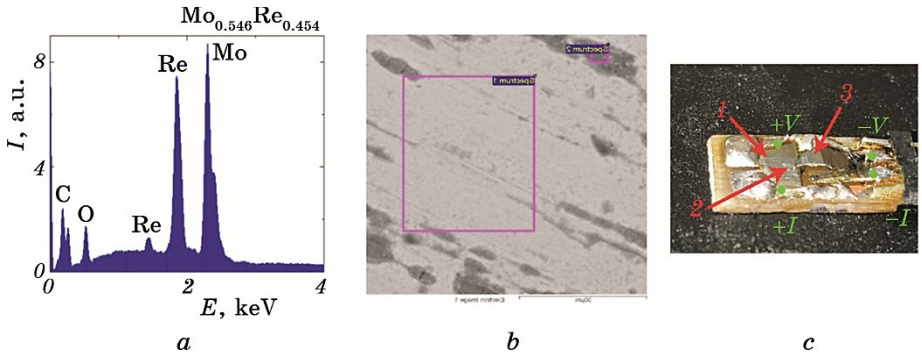

Fig. 1. Energy spectrum with signatures of specific chemicals elements for superconductor alloys MoRe (*a*), surface of the scanned area in MoRe alloy, dark areas correspond to an oxidized surface (*b*), *S*–*N* type (MoRe–Ni) point contact: *1*—Ni plate, *2*—a point contact between Ni plate and MoRe tip, *3*—MoRe tip (*c*).

changed the configuration of the heterostructure under study, using the Mo–Re alloy tip as a counter-electrode for a Ni plate (Fig. 1, *c*). The created contact configuration made it possible to carry out true 4-point measurements for temperatures below the critical temperature of the Mo–Re alloy. The partial composition of the $Mo_{0.546}Re_{0.454}$ alloy was determined using the energy spectrum (Fig. 1, *a*). The SEM image has shown the dark areas oxidized surface of Mo–Re alloy (Fig. 1, *b*).

In strong ferromagnets such as Ni, the exchange energy E_{ex} is of the order of several hundreds of meV (see, for example, the band structure calculations for ferromagnetic Ni in [20], which revealed exchange splitting of the *d* band between 0.22 and 0.36 eV that results in the spin polarization efficiency about 35%). The relative energy shift of the subbands with different electron spins strongly reduces pairing correlations entering the *F* layer from the *S* side. Related estimates performed in Ref. [21] have found that the penetration length ξ_F of the superconducting condensate into the ferromagnetic Ni is extremely short and does not exceed 1 nm.

3. FABRICATION OF Mo–Re/Ni CONTACTS AND THEIR MEASUREMENTS

Extremely low oxidability of the molybdenum–rhenium alloy is well established and caused great problems in creating tunnel barriers on the surface of Mo–Re samples in a natural way [22, 23]. However, for the point-contact spectroscopy, this restriction is extremely useful since it makes it possible to study the spectrum of quasi-particle excitations directly in the near-contact region that is especially important for hetero-

structures formed by the Mo–Re alloy with ferromagnets with $\xi_F < 1$ nm.

The contacts between the Mo–Re tip and the Ni plate were created in the following way. A thin Mo–Re alloy plate with a tip at the end was pressed to a Ni thick plate. Two contacts were connected to the Mo–Re alloy plate with the tip. Two independent contacts were also connected to the Ni plate. A 4-point measurement scheme was implemented (Fig. 1, *c*). The clamping force determined the contact resistance. Thus, we have measured current–voltage characteristics $I(V)$ and the differential conductance spectra $G_S(V) = dI(V)/dV$ using the conventional four-probe configuration [24] (see the inset in Fig. 3).

Simultaneous measurements of the direct and differential current–voltage characteristics of point contacts was carried out using a digital Lock-in Amplifier SR830, which also set the alternating component of the sinusoidal current through an *I* Source (Fig. 2). The same converter, receiving bias voltage from a digital-to-analog converter (DAC), generated a stable direct current component. Thus, there was a stepwise change in the DC component of the current with constant amplitude of the AC component ($I_{bias} + I_{ac}$). The measurements were made at a frequency of 9.777 KHz. AC current amplitude was $I_{ac} = 20$ μA. Low-pass filters separate the DC component of the signal. In this way, the direct and differential current–voltage characteristics were measured simultaneously. A similar measurement scheme has proven itself to be effective in detecting terahertz radiation [25, 26], Fraunhofer modulation [27], detecting subharmonic Shapiro steps [28] in low-resistance Josephson junctions, to obtain the first and second derivatives of tunnel current–voltage characteristics [23], precision resistance measure

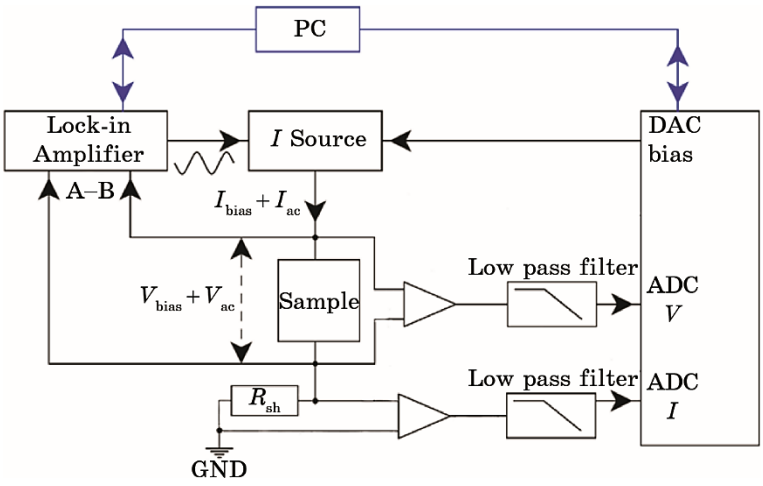

Fig. 2. Scheme for measuring the direct and differential current–voltage characteristics.

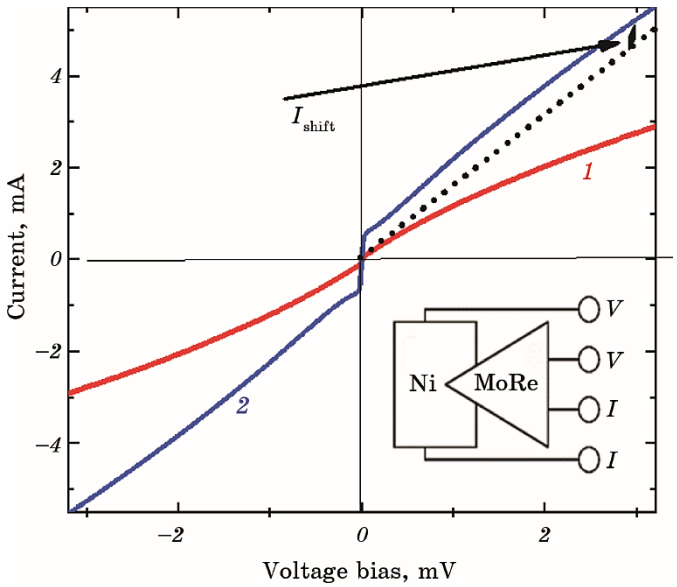

Fig. 3. Relatively small variations in the pressing of the Mo–Re alloy tip into the Ni film lead to small changes in the contact resistance from 1.42 Ω (dashed line) to 0.70 Ω (solid line), but radical alterations in the current–voltage curves. The dotted line demonstrates the presence of the excess current I_{exc} in the latter characteristic. The inset shows a 4-point measurement scheme.

[29], when the analysis of current–voltage characteristics is directly complicated by the presence of large noise in relation to small changes in the signal.

In the case of a single-band superconductor, the general formula for calculating the ratio of differential conductance in superconducting and normal states reads as [30]:

$$\frac{G_S(V)}{G_N} = 1 + \frac{1 + D_N\left|\gamma(E)\right|^2 - R_N\left|\gamma^2(E)\right|^2 - \left|1 - R_N\gamma^2(E)\right|^2}{\left|1 - R_N\gamma^2(E)\right|^2}. \qquad (1)$$

Here, the parameter Z determines the probability of electron transmission through the interface $D_N = 1/(1+Z^2)$ in the normal state as well as the reflection probability $R_N = 1 - D_N = Z^2/(1+Z^2)$, $E = eV$, $\gamma(E) = \Delta(E) / (E + (E^2 - \Delta^2(E))^{1/2})$, the normal conductivity G_N is proportional to the D_N magnitude. It is convenient to introduce a constant imaginary part in the electronic energy $E \to E + i\Gamma$ with the Dynes parameter Γ that takes into account the effects of inelastic-scattering processes and temperature.

Hence, in a single-band superconductor, we have three adjustable parameters: the energy gap Δ, the interface scattering efficiency Z,

and the parameter Γ. When we are dealing with a two-band superconductor, their number doubles and a seventh parameter is added, which specifies the relative contribution of the two bands to the final result: Δl, Δs, Z_l, Z_s, Γ_l, Γ_s and the weighting factor $w_l < 1$ ($w_s = 1 - w_l$):

$$G(V) = w_l G_l(V) + w_s G_s(V). \quad (2)$$

4. MAIN RESULTS AND DISCUSSION

We started by proving a high sensitivity of the contacts between the two-gap superconductor and a strong ferromagnet to the interface properties is shown in the representative Fig. 3.

Let us analyse the curve *2* in Fig. 3 using the expression fir the excess current $I_{\text{exc}} = 4\Delta/3eR_N$ obtained in the paper [31] we get the value $\Delta = 0.55$ meV that can be considered as an average value of the energy gap after the two-band Mo–Re superconductor approaches the ferromagnetic Ni. Let us check this conclusion by comparing the experimentally measured dependence of the differential resistance $dV/dI_S(V)$ on the applied bias voltage V with the theoretically expected formula (1). The obtained parameters are given in the caption to Fig. 4. Obviously, there is a suppression of two energy gaps, which affects the smaller gap more strongly. Apparently, this is a consequence of the discrepancy between the band parameters of the ferromagnetic Ni elec-

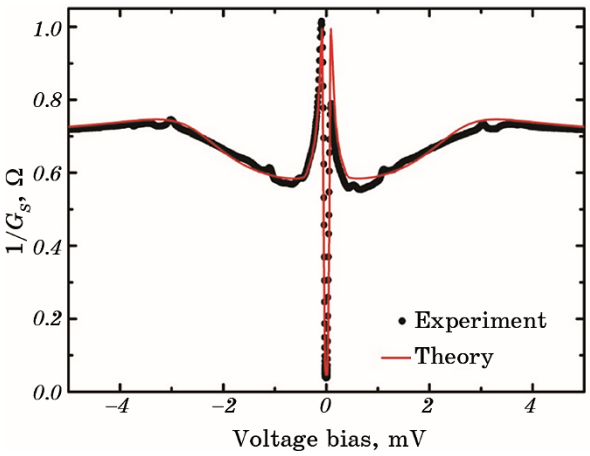

Fig. 4. Differential resistance $1/G_S(V) = dV/dI_S(V)$ for the sample whose I–V curve is shown in Fig. 3 as line *2*. In the normal state, $G_N = 1.43S$. The contact parameters Z and Γ for two electron bands differ significantly from each other: $Z_s = 1.9$, $Z_l = 1.4$, $\Gamma_s = 0.015$, $\Gamma_l = 1.1$ as well as the energy gaps $\Delta_s = 0.08$ meV and $\Delta l = 0.65$ meV, partial contributions of the bands $w_s = 0.4$ and $w_l = 0.6$, the measurement temperature was of 4.2 K.

trode and the corresponding electron band in the Mo–Re alloy, which is responsible for the larger gap Δl. The asymmetry of the peaks in Fig. 4 can be associated with the dependence of the positive and negative critical current on the contact's own field, which is induced by the transport current, as well as with the magnetic flux trapped nearby [28].

5. SUMMARY

For the first time, we have created and studied electrical characteristics of a point contact between the two-band/two-gap superconductor, the Mo–Re alloy, and the strong ferromagnet, Ni. In agreement with the theory [15], we have found that small variations in the contact resistance caused by pressing the Mo–Re tip against the Ni film led to radical changes in the current–voltage characteristics. Unexpectedly, the proximity effect of Ni noticeably differs for the two bands in the Mo–Re alloy while the small gap opened at the main band is strongly suppressed by the presence of a nearby ferromagnetic, the large gap experiences not so big changes. We believe that it is emerging at a new small band that opens at low Re concentrations and strong discrepancy between the corresponding momenta in the Mo–Re alloy and ferromagnetic Ni prevents intensive exchange of electrons between them, see also the work [9]. In our opinion, additional experiments aimed to study quantum noise in such systems [32] may shed light on this issue.

This work was carried out within the framework of the project 2020.02/0408 funded by the National Research Foundation of Ukraine.

REFERENCES

1. H. Suhl, B. T. Matthias, and L. R. Walker, *Phys. Rev. Lett.*, **3**: 552 (1959).
2. A. J. Leggett, *Prog. Theor. Phys.*, **36**: 901 (1966).
3. G. Binnig, A. Baratoff, H. E. Hoenig, and J. G. Bednorz, *Phys. Rev. Lett.*, **45**: 1352 (1980).
4. C. Ren, Z. S. Wang, H. Q. Luo, H. Yang, L. Shan, and H. H. Wen, *Phys. Rev. Lett.*, **101**: 257006 (2008).
5. V. Cvetkovic and Z. Tesanovic, *Europhys. Lett.*, **85**: 37002 (2009).
6. V. Tarenkov, A. Dyachenko, V. Krivoruchko, A. Shapovalov, and M. Belogolovskii, *J. Supercond. Nov. Magn.*, **33**: 569 (2020).
7. V. Tarenkov, A. Shapovalov, O. Boliasova, M. Belogolovskii, and A. Kordyuk, *Low Temp. Phys.*, **47**: 101 (2021).
8. V. Tarenkov, A. Shapovalov, E. Zhitlukhina, M. Belogolovskii, and P. Seidel, *Low Temp. Phys.*, **49**: 103 (2023).
9. H. Zhang, Q. Yang, Q. Dai, K. Linghu, R. Nie, and F. Wang, *Supercond. Sci. Technol.*, **27**: 055020 (2014).
10. V. N. Krivoruchko and V. Yu. Tarenkov, *Phys. Rev. B*, **75**: 214508 (2007).

11. V. N. Krivoruchko and V. Yu. Tarenkov, *Phys. Rev. B*, **78**: 054522 (2008).
12. V. Krivoruchko and V. Tarenkov, *Phys Rev B*, **86**: 104502 (2012).
13. X. Liu , R. P. Panguluri, R. Mukherjee, D. Mishra, S. Pokhrel, D. P. Shoemaker, Z.-F. Huang, and B. Nadgorny, *Phys. Rev. B*, **106**: 224417 (2022).
14. M. A. Belogolovsskii, Yu. F. Revenko, A. Yu. Gerasimenko, V. M. Svistunov, E. Hatta, G. Plitnik, V. E. Shaternik, and E. M. Rudenko, *Low Temp. Phys.*, **28**: 391 (2002).
15. R. Grein, T. Löfwander, G. Metalidis, and M. Eschrig, *Phys. Rev. B*, **81**: 094508 (2010).
16. F. Pérez-Willard, J. C. Cuevas, C. Sürgers, P. Pfundstein, J. Kopu, M. Eschrig, and H. V. Löhneysen, *Phys. Rev. B*, **69**: 140502(R) (2004).
17. L. S. Sharath Chandra, S. Sundar, S. Banik, S. K. Ramjan, M. K. Chattopadhyay, N. Jha, and S. B. Roy, *J. Appl. Phys.*, **127**: 163906 (2020).
18. N. A. Tulina and S. V. Zaitsev, *Solid State Commun.*, **86**: 55 (1993).
19. S. Sundar, L. S. S. Chandra, M. K. Chattopadhyay, and S. B. Roy, *J. Phys.: Condensed Matter*, **27**: 045701 (2015).
20. W. Nolting, W. Borgiel, V. Dose, and Th. Fauster, *Phys. Rev. B*, **40**: 5015 (1989).
21. I. P. Nevirkovets and M. A. Belogolovskii, *Supercond. Sci. Technol.*, **24**: 024009 (2011).
22. J. Talvacchio, M. A. Janocko, and J. Greggi, *J. Low Temp. Phys.*, **64**: 395 (1986).
23. A. D'yachenko, A. Kalenyuk, V. Tarenkov, A. Shapovalov, O. Boliasova, and D. Menesenko, *Low Temp. Phys.*, **49**: 209 (2023).
24. M. Poláčková, E. Zhitlukhina, M. Belogolovskii, M. Gregor, T. Plecenik, and P. Seidel, *Eur. Phys. J. Plus*, **138**: 486 (2023).
25. R. Cattaneo, E. A. Borodianskyi, A. A. Kalenyuk, and V. M. Krasnov, *Phys. Rev. Applied*, **16**: L061001 (2021).
26. M. M. Krasnov, N. D. Novikova, R. Cattaneo, A. A. Kalenyuk, and V. M. Krasnov, *Beilstein J. Nanotechnol.*, **12**: 1392 (2021).
27. A. A. Kalenyuk, A. Pagliero, E. A. Borodianskyi, A. A. Kordyuk, and V. M. Krasnov, *Phys. Rev. Lett.*, **120**: 067001 (2018).
28. A. A. Kalenyuk, E. A. Borodianskyi, A. A. Kordyuk, and V. M. Krasnov, *Phys. Rev. B*, **103**: 214507 (2021).
29. A. A. Kalenyuk, A. Pagliero, E. A. Borodianskyi, S. Aswartham, S. Wurmehl, B. Büchner, D. A. Chareev, A. A. Kordyuk, and V. M. Krasnov, *Phys. Rev. B*, **96**: 134512 (2017).
30. D. Daghero and R. S. Gonnelli, *Supercond. Sci. Technol.*, **23**: 043001 (2010).
31. G. E. Blonder, M. Tinkham, and T. M. Klapwijk, *Phys. Rev. B*, **25**: 4515 (1982).
32. E. Zhitlukhina, M. Belogolovskii, and P. Seidel, *Appl. Nanosci.*, **10**: 5121 (2020).